TELKOMNIKA Indonesian Journal of Electrical Engineering
Vol.12, No.7, July 2014, pp. 5022 ~ 5036
DOI: 10.11591/telkomnika.v12i7.4709

A Novel SSR Mitigation Method Based on GCSC in DFIG with Series Connected Compensator

Zakieldeen Elhassan[1], Li Yang*[2], Tang Yi[3]
School of Electrical Engineering, Southeast University,
China, Jiangsu, Nanjing 210096
*Corresponding author, e-mail: zakideenzain@gmail.com[1], li_yang@seu.edu.cn[2], tangyi@seu.edu.cn[3]

Abstract

This paper presents a novel study for SSR mitigating in the wind power systems based on DFIG using GCSC (Gate controlled series capacitor). The GCSC is composed of three pairs of anti-parallel GTO Thyristors (Gate Turn- off) connected in parallel with a fixed capacitor. The GCSC is applied to reduce inrush current in capacitor compensator during the transient operation by executing a proper firing angle control of thyristor gates. In order to realize SSR oscillation when the transient operation occurred, the DFIG turbine is connected through the shaft turbine model. The simulation results shown that the GCSC device is suitable and reasonable for suppressing SSR caused by torsional interaction (TI) and torque amplification (TA) and also damping the subsynchronous oscillation as well. The transient simulations have been carried out using PSCAD/EMTDC program to demonstrate the capability of the GCSC device in mitigating SSR.

Keywords*: subsynchronous resonance SSR, series capacitor compensator, vector control method, doubly fed induction generator DFIG, interpolated firing pulse*

1. Introduction

SSR phenomenon might take place in the system with a series compensated transmission line when the transient operation happened in the power system. Because, the interaction between the series compensated network electrical oscillation, and the mechanical oscillation of the generator drive train produces torsional torques. This torsional torque may be led to the shaft fatigue when the system has transient mode operations. Therefore, SSR mitigation has gotten more attention and significant care study in order to avoid the problems associated with SSR, and it continues to be a subject of research and development. Referring to that, many studied are done in SSR mitigation, especially when the DFIG was employed as the generator in wind energy. The basic study of the SSR quantitie's calculation and tests is presented in [1]. The work [2] discusses clearly the DFIG control strategy using the voltage command in the control loops of the grid side converter (GSC) to damping SSR. Moreover, the SSR definition, classification and mitigation have got great interest in various papers such as [3-5].

Recently, the SSR mitigation using flexible AC transmission systems (FACTS) in the series-compensated wind energy has been demonstrated in the literature. These FACTS devices include the static synchronous series compensator (SSSC), thyristor-controlled series capacitor (TCSC), static var compensator (SVC) and (STATCOM). In a modern paper [6] the SSR study modified IEEE first benchmark model is mitigated by using SSSC. Even though, the more recently research was oriented to SSR damping using the subsynchronous current suppressor with the SSSC [7]. The TCSC is applied in many modes of SSR suppression study either in the frequency scanning or impedance method as in [8-10]. Moreover, the TCSC has useful application in the damping of SSR study exactly in the scanning frequency method [11]. The applying of SVC in the SSR damping has been implemented and discussed in [12]. Both [13] and [14] explained a novel control for mitigating SSR in the wind farm and wind park with series compensated by using STATCOM controller.

On the other hand, the GCSC device presents as new FACTS devices for series compensation of transmission lines study as in [15]. Up to now, the GCSC is rarely applied to mitigate subsynchronous resonance, unless some researchers focus their researches in this

Received October 11, 2013; Revised March 11, 2014; Accepted March 26, 2014

field. Among them, the Jesus et al. [16] presented the SSR mitigation using GCSC device, and they were applied IEEE first benchmark model to test the GCSC operation. In this study, the GCSC gate control is achieved by a zero-crossing detector, which uses the system power as a feedback signal control instead of the frequency deviation. Additionally, this study was obtained a good result, but it needs more specific control in the GCSC firing angles.

It's demonstrated that all devices applied in SSR analysis and damping to enhance the power system stability and control are mitigated SSR problems, but they have some limited applications. For example, the TCSC has some disadvantages like it generates a new reactance between the capacitor, and thyristor controlled reactance at the normal frequency for known blocking angle of the thyristor. Furthermore, the variation of reactance in the TCSC is slightly narrow [15]. The SSSC compensator has useful application, but the cost is very high because it includes converters inside.

Therefore, this paper presents the GCSC with simple construction and flexible operation to achieve SSR suppression in the wind power system based on DFIG with the series-compensated transmission line. This research considers SSR study using one of the SSR analytical tools, namely is an electromagnetic Transients Program (EMTP). The EMTP is a program for numerical integration of the system differential equations and its suitable for SSR study in dynamic operation. The SSR phenomenon was discussed throughout the system model study with and without GCSC device. The results show that the GCSC has been able to alleviate the SSR problems and improve subsynchronous oscillations.

2. SSR Definition

SSR is a dynamic event of attention in power systems that have certain special characteristics. The formal definition of SSR provides by the IEEE as an electric power system condition where the electric network exchanges energy with a turbine generator at one or more natural frequencies of the combined system below the synchronous frequency of the system [17]. The definition includes any system condition that provides the opportunity for an exchange of energy at a given subsynchronous frequency. The most common example of the natural mode of subsynchronous oscillation is due to the series capacitor compensated transmission lines. These lines, with their series LC combinations, have natural frequencies are defined by:

$$f_n = \frac{1}{2\pi}\sqrt{\frac{1}{LC}} = f_b\sqrt{\frac{X_C}{X_L}} \quad (1)$$

Where f_n is the SSR frequency associating with LC transmission, f_b is the base frequency and X_L, X_C are the inductive and capacitive reactances, respectively. The f_n in the SSR frequency which has a corresponding component induced in the rotor circuits with the frequency $(f_n - f_m)$, f_m is the frequency of rotating speed. So in this study, the SSR frequency considers is $(f_n - f_b)$ which directly related to the network interaction with series compensator. Thus, the effective transmission impedance X_{eff} with series capacitive compensation is given as:

$$X_{eff} = X - X_C = (1 - K)X \quad (2)$$

Where X is the total line reactance, and K is the degree of series compensation, $K = \frac{X_C}{X}$, $0 \leq K < 1$, and K usually between 25% to 75%.

SSR is a resonant condition, with frequencies below the nominal frequency, which is related to an energy exchange between the electrical and the mechanical system, coupled through the generator. The SSR can be divided into two main particular groups [9, 18]:

1. Steady state SSR includes: Induction generator effect (IGE) and torsional interaction (TI)
2. Transient torques or torque amplification (TA).

The IGE is rarely happened in the series compensated power systems. However, the SSR caused by TI and TA are dangerous conditions that must be avoided in power systems and usually happens in series compensated power systems.

3. System Studied Model

The configuration of the studied system has been shown in Figure 1. This figure, is basically modified from the IEEE first benchmark model as in [19]. It consists of wind turbine based on DFIG with back to back converters, transformer, power grid and series compensated transmission line. The parameter data of DFIG are arranged as in table I and it's taken from the [20]. The DFIG shaft system consists of three masses: a high pressure turbine (HP) to represent turbine blades, an intermediate stage pressure turbine (IP) (gearbox) and a low pressure turbine (LP) (hub). All masses are mechanically connected together using elastic shafts. The DFIG and converters are protected by voltage limits and an over-current 'crowbar' circuit. The converter system enables variable speed operation of the wind turbine by de-coupling the power system electrical frequency and the rotor mechanical frequency. To study SSR mitigation, the GCSC device is connected in series with a transmission line to reduce the transient voltage through the capacitor by inserting the GCSC capacitor when the system has a dynamic mode by applying proper firing angle control.

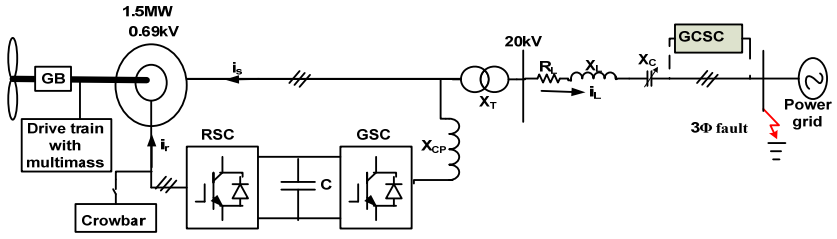

Figure 1. Studied System Configuration

4. Wind Power Expression

The wind turbine mechanical output power is given by [21-24]:

$$P_m = \frac{1}{2}\rho\pi R^2 C_p(\beta, \lambda) V_w{}^3 \quad (3)$$

Where P_m is the mechanical extraction wind power, ρ is the air density (1.225kg/m^3), R is the rotor radius, V_w is the wind speed in m/s, λ is the tip speed ratio, β is the blade pitch angle in degree (β is usually set as 0 for the maximum value of C_p), C_p is the power coefficient as a function of both tip-speed ratio λ and the blade pitch angle β. The tip speed ratio λ, defined by:

$$\lambda = \frac{R\Omega_M}{V_w} \quad (4)$$

Here Ω_M is the turbine rotor speed (rad/s) at a specific wind speed (m/s). The theoretical maximum value of C_p is given by the Betz's limit, (about 0.593) [25]. But there are many numerical equations have been developed to calculate the C_p for identified values of λ and β as in [24].

$$C_p(\lambda, \beta) = 0.73\left(\frac{151}{\lambda_j} - 0.58\beta^{2.14} - 13.2\right) e^{\frac{-18.4}{\lambda_j}} \quad (5)$$

Where,

$$\lambda_j = \frac{1}{\frac{1}{\lambda - 0.02\beta} - \frac{0.003}{\beta^3 + 1}} \quad (6)$$

According to these equations mentioned above, the pitch angle control is built inside of the PSCAD wind turbine package to achieve maximum wind turbine torque and controller data is set in Table 2.

5. DFIG Mathematical Model

The DFIG stator and rotor voltage equations referring to the direct and quadrature (dq) reference frame can be written as [20], [26-27]:

$$V_{ds} = R_s i_{ds} + p\lambda_{ds} - \omega_s \lambda_{qs}\,; \quad V_{qs} = R_s i_{qs} + p\lambda_{qs} + \omega_s \lambda_{ds} \tag{7}$$

$$V_{dr} = R_r i_{dr} + p\lambda_{dr} - (\omega_s - \omega_r)\lambda_{qr}\,; \quad V_{qr} = R_r i_{dr} + p\lambda_{qr} + (\omega_s - \omega_r)\lambda_{dr} \tag{8}$$

Here p is the derivative $\frac{d}{dt}$, ω_s is synchronous speed, ω_r is rotor speed and the term $(\omega_s - \omega_r)$ is defined as slip speed ω_{SL}.

The d&q axes flux in both stator and rotor ($\lambda_{ds}, \lambda_{qs}$, λ_{dr} and λ_{qr}) are very difficult to estimate these parameters, so these fluxes can be written with the stator and rotor inductances. Regarding to that, the DFIG dynamic equations are written as [25]:

$$\begin{cases} pi_{ds} = D\left[L_r v_{ds} - L_m v_{dr} - R_s L_r i_{ds} + (D\omega_s + \omega_r L_m^2) i_{qs} + R_r L_m i_{dr} + \omega_r L_r L_m i_{qr}\right] \\ pi_{qs} = D\left[L_r v_{qs} - L_m v_{qr} - R_s L_r i_{qs} - (D\omega_s + \omega_r L_m^2) i_{ds} + R_r L_m i_{qr} - \omega_r L_r L_m i_{dr}\right] \\ pi_{dr} = D\left[L_s v_{dr} - L_m v_{ds} + R_s L_m i_{ds} + (D\omega_s - \omega_r L_s L_r) i_{qr} - R_r L_s i_{dr} - \omega_r L_s L_m i_{qs}\right] \\ pi_{qr} = D\left[L_s v_{qr} - L_m v_{qs} + R_s L_m i_{qs} - (D\omega_s - \omega_r L_s L_r) i_{dr} - R_r L_s i_{qr} + \omega_r L_s L_m i_{ds}\right] \end{cases} \tag{9}$$

Where,

$$D = \frac{1}{L_r L_s - L_m^2} \tag{10}$$

The stator and rotor voltages and currents can be calculated as:

$$\vec{V}_s = V_{ds} + jV_{qs},\ \vec{V_r} = V_{dr} + jV_{qr},\ \vec{i}_s = i_{ds} + ji_{qs} \text{ and } \vec{i}_r = i_{dr} + ji_{qr} \tag{11}$$

The stator active power P_s and reactive power $Q_s$are given by:

$$P_s = \frac{3}{2}\left(V_{ds} i_{ds} + V_{qs} i_{qs}\right);\quad Q_s = \frac{3}{2}\left(V_{qs} i_{ds} - V_{ds} i_{qs}\right) \tag{12}$$

Here, the quadrature stator voltage V_{qs} set to 0, so that the Equation (12) rewritten as:

$$P_s = \frac{3}{2}(V_{ds} i_{ds});\quad Q_s = -\frac{3}{2}\left(V_{ds} i_{qs}\right) \tag{13}$$

The motion and electromagnetic torque equations are given by:

$$\begin{cases} T_e = \frac{3PL_m}{2}\left(i_{qs} i_{dr} - i_{ds} i_{qr}\right) \\ p\omega_r = \frac{P}{J}(T_e - T_m) \end{cases} \tag{14}$$

Where P is the number of pole pairs.

6. DFIG Converters Control

Generally, the DFIG model contains a back-to-back converter based on two-level converters. The two- level converters are modelled with ideal switches that allow current flows in both directions. In this exposition, the controlled semiconductor with a diode in anti-parallel used is an insulated gate bipolar transistor (IGBT). The DFIG converters control is adopted by using a vector control method as in the [20, 26]. The vector control method is deeply applied in the grid side converter GSC and rotor side converter RSC. The [28] presents a new proposed method of

DFIG vector control based on the inverse system and variable structure sliding mode(VSS). The RSC is used to regulate the slip power in order to control the generator speed and torque while the GSC maintains a constant DC link voltage in the grid side. The GSC is in charge of controlling part of the power flow of the DFIG. This power is incompletely delivered through RSC, DC link and finally is transmitted by the GCS to the grid [25], [29-30]. There are many control strategies of GSC when it's applied in the DFIG wind turbine, and the most model of this purpose can be found in the [31]. However, in this paper, the comprehensive equations to get the reference values of the GSC and RSC are written based on [20, 25] as below,

$$\begin{cases} V_{ds}^{ref} = [(V_{dc}^{ref} - V_{dc})\left(K_{pdc} + \frac{K_{idc}}{s}\right) - i_{ds}]\left(K_{pds} + \frac{K_{ids}}{s}\right) - i_{qs}X_T \\ V_{qs}^{ref} = \left(i_{qs}^{ref} - i_{qs}\right)\left(K_{pqs} + \frac{K_{iqs}}{s}\right) - i_{ds}X_T \end{cases} \quad (15)$$

$$\begin{cases} I_{rd}^{ref} = (Q_g^{ref} - Q_g)\left(K_{pdr} + \frac{K_{idr}}{s}\right) \\ I_{rq}^{ref} = (\omega_m - \omega_{ref})\left(K_{pqr} + \frac{K_{iqr}}{s}\right) \end{cases} \quad (16)$$

The q-axis current reference i_{qs}^{ref} can be obtained from:

$$i_{qs}^{ref} = -\frac{Q_s}{1.5V_{ds}} \quad (17)$$

Where the K_{pdc}, K_{pds}, K_{pqs}, K_{pdr}, K_{pqr} and K_{idc}, K_{ids}, K_{iqs}, K_{idr}, K_{iqr} are proportional and integral gains of DC link voltage, stator and rotor direct and quadrature currents respectively. These parameters are playing a great role in enhancing the voltage control. Thus, the values are designed according to system components and DFIG parameters to realize specify control of converters in both sides. The X_T is the coupling transformer reactance and the Q_g^{ref} is the grid reactive power which is set to zero value.

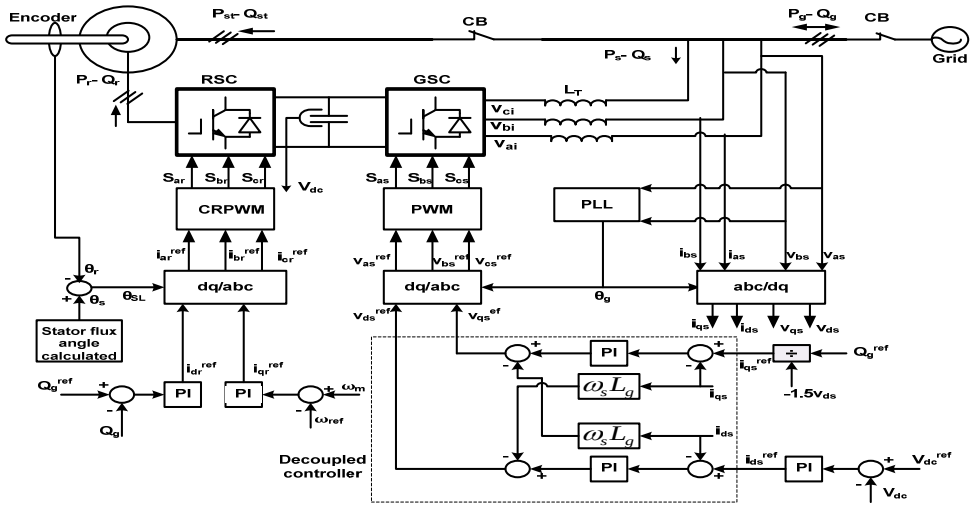

Figure 2. DFIG GSC and RSC Block Diagram Control

7. Shaft Model Equations

The shaft model in this study is assumed as an elastic multimass model with four masses including the DFIG. This model can be graphically shown in Figure 3. The shaft model is represented by linear mathematical equations and the masses are selected as three masses according to the reference [33]. The mathematical equations of the turbine-generator referring to the [34, 35] are written as:

$$2H_1\frac{d\omega_1}{dt} + K_{12}(\delta_1 - \delta_2) + D_{12}(\omega_1 - \omega_2) = T_1 \quad (18)$$

$$2H_2\frac{d\omega_2}{dt} + K_{12}(\delta_2 - \delta_1) + K_{23}(\delta_2 - \delta_3) + D_{12}(\omega_2 - \omega_1) + D_{23}(\omega_2 - \omega_3) = T_2 \quad (19)$$

$$2H_3\frac{d\omega_3}{dt} + K_{23}(\delta_3 - \delta_2) + K_{34}(\delta_3 - \delta_4) + D_{23}(\omega_3 - \omega_2) + D_{34}(\omega_3 - \omega_4) = T_3 \quad (20)$$

$$2H_g\frac{d\omega_g}{dt} + K_{34}(\delta_4 - \delta_3) + D_{34}(\omega_4 - \omega_3) = T_m - T_e \quad (21)$$

Where H is the inertia constant of each turbine blade in sec, K is the spring constant in N.m/rad, ω is the mechanical speed in rad/sec, D is the mutual damping in N.m-s/rad, δ is the rotor angle in rad, T_m is the mechanical torque in N.m and T_e is the electromagnetic torque in N.m. We notice here the masses self-damping are omitted from these equations for linearizing. In additional, the common dynamic equation of the generator- turbine model could be written in second order equation to ith row as:

$$J_i\ddot{\delta}_i + K_i\dot{\delta}_i + D_i\delta_i = T_i \quad (22)$$

$$J_i = 2H_i \quad (23)$$

Where i = 1, 2, 3 , here (i) is the number of masses.

If we compare the equation (22) with standard second order equation solutions, we get natural frequencies of the shaft model as:

$$f_i = \frac{1}{2\pi}\sqrt{\frac{K_i}{2H_i}} \quad (24)$$

The Equation (24) is used to obtain the shaft model parameters when the natural frequency of the shaft model is known. However, in this study, the eigenvalue method is used to obtain the masses natural frequencies by using the Matlab program. From the imaginary parts of eigenvalues, the multimass natural frequencies namely are calculated as: 10.64, 21.102 and 29.523Hz respectively. The shaft model system data are modified from IEEE first benchmark and listed in Table 3.

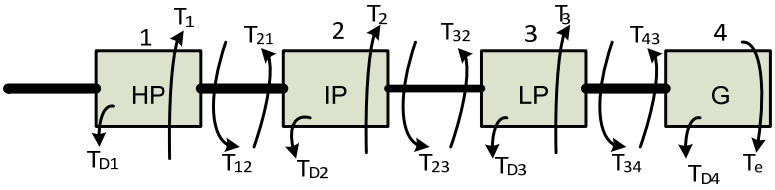

Figure 3. Equivalent Shaft Model Diagram

8. GCSC Device

The GCSC consists of a fixed capacitor in shunt with GTO thyristor has the capabilities to turn on and off upon control action. The GCSC is applied to control voltage across the capacitor at given line current by using GTO valves, according to the gate open and close. The capacitor is bypassed when the valve is closed and when it opens the current is followed through the capacitor. Furthermore, the bidirectional GTO thyristors have a parallel snubber capacitor circuit to execute the system protection [20]. Figure 4 shows the GCSC basic circuit topology with compensator transmission line elements. The main goal of using a GCSC device is to mitigate the SSR problems by reducing inrush current caused by the transient operation that takes place when the three phase fault occurs in the system. GCSC has the same work action with TSSC (thyristor- switched series capacitor) which applies to control the AC voltage through capacitor at the given line current [36]. However, the difference between two

models that the TSSC uses thyristor and the GCSC uses the gate turn-off thyristor (GTO). Furthermore, the GCSC has been able to vary the reactance from zero to the maximum compensation related to the fixed capacitor value. The GCSC must be operated with proper GTO firing angle control which automatically closes and open according to control action. So the equation of GCSC could be written referring to [15], [16], [36] and [37] as:

$$V_C(\alpha) = \frac{1}{C}\int_{\alpha}^{\omega t} I\cos(\omega t)\, dt = \frac{I}{\omega C}[\sin\omega t - \sin\alpha] \quad (25)$$

Where $V_C(\alpha)$ is the voltage across the capacitor, I is the maximum value of line current and α is the thyristor firing angle which interval is $\alpha \le \omega t \le \pi - \alpha$. The turn-off angle(α) is measured from the zero crossing of the line current and the compensation level of the GCSC is determined by the fundamental component of the voltage $V_C(\alpha)$ on the GCSC. The GCSC reactance varies from maximum value at $\alpha = \frac{\pi}{2}$ radian to zero value for $\alpha = \pi$ radian [37, 38]. Referring to that, the equivalent reactance of the GCSC as a function of α can be expressed as:

$$X_C(\alpha) = \frac{X_C}{\pi}[2\alpha - 2\pi - \sin 2\alpha] \quad (26)$$

According to the Equation (26) the reactance of the capacitor can be changed to various values related to the firing angle of thyristor, but we notice here all the reactance values must be positive value, so that the firing angle usually less than π. Figure 5 shows the impedance value per unit of the GCSC as a function of the firing angle(α) and Figure 6 graphically explained the relationship between the capacitor voltage and turn-off delay angle.

In order to control the GCSC operation, the appropriate firing angle circuit is designed to enable the thyristor gate conducting or not conduct. Thereby the interpolated firing pulse is applied to release the GTO Thyristors gate enable after receiving the alpha angle(α) from the phase locked loop (PLL). The phase locked loop PI controller gains are obtained by using trial and error method. This PLL generates a ramp signal of angle(α) variation between (0 and 360°), synchronized or locked in phase, to the input voltage V_{th} which is measured across the capacitor. The initial angle(α_0) adjusted to suitable value, then it compares with ramp signal (α) in the interpolated firing pulse to enable thyristor operation. Figure 7 shows the control scheme model of GCSC. Hence, the GCSC can be operated in voltage control or compensating reactance control according to the applied control.

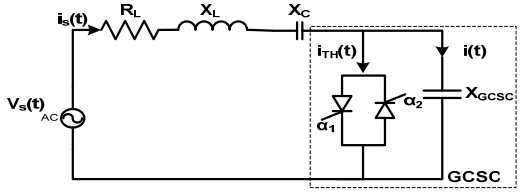

Figure 4. GCSC Equivalent Circuit with Compensator Line Parameters

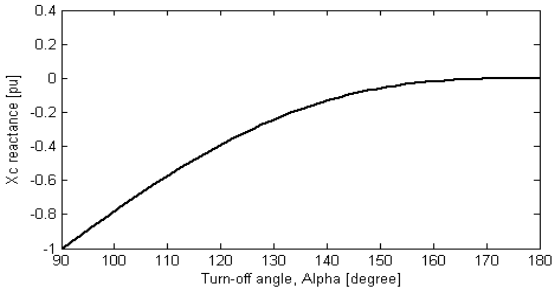

Figure 5. GCSC Impedance as a Function of Angle(α)

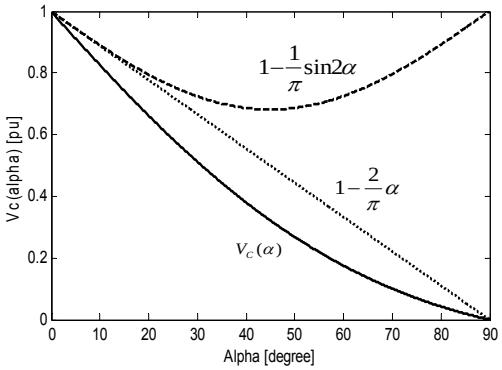

Figure 6. Fundamental Component of the Series Capacitor Voltage Against Turn-off Delay Angle

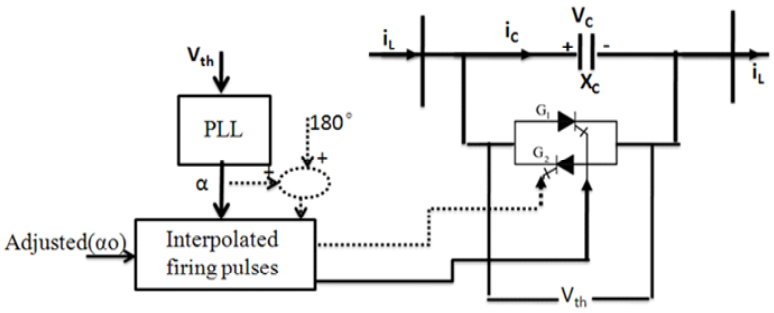

Figure 7. Scheme Control Model of the GCSC

9. Simulation Results and Discussion

Figure 1 is used to verify the SSR mitigation based on the GCSC, and the system model was constructed and implemented in the PSCAD program. Initially, the system is running under steady state and 3Φ fault occurred at 8sec with duration time 0.11sec. The GCSC is connected in series with the compensated transmission line to mitigate SSR effects due to transient mode occurrence in the power system. The adjusted firing angle of GCSC is set to the computed value ($\alpha_0 = 60°$).

Under the above circumstances, series comparative results with and without GCSC have been plotted from the PSCAD & MATLAB to describe system behavior.

The DFIG stator real and reactive powers are viewed in Figure 8(a) and (b). As we have seen in Figure 8(a) without GCSC, the P_s during the fault is decreased to a negative value and after fault clearing does not return to the same value before transient mode which indicates that the system lost synchronism and this leads to unstable operation. Whilst with GCSC, the P_s characteristic curve transient is more safety because the GCSC produced a necessary required power to compensate system reactive power during dynamic mode to prevent the SSR occurred. Figure 8(b) is clearly shown the stator reactive power Q_s which with GCSC is more linear and stable. This indicates that the GCSC changes the system reactance to new value by adding the GCSC reactance X_{GCSC}. These results are confirmed again in the DFIG active and reactive powers, which are shown in Figure 9(a) and (b) respectively. The DFIG reactive power with GCSC is always maintained to zero to ensure a DFIG unity power factor which is directly improved voltage stability control.

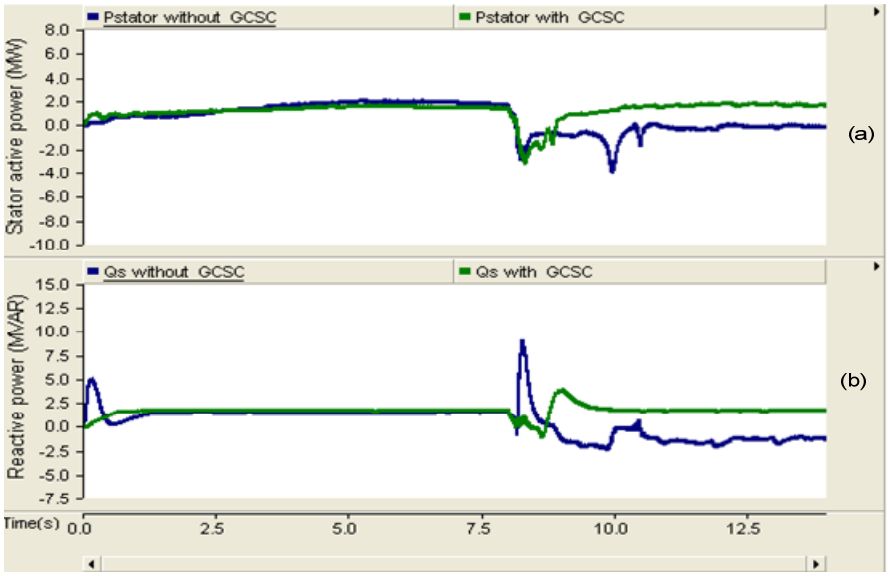

Figure 8. Stator Power Response: (a) active power, (b) reactive power

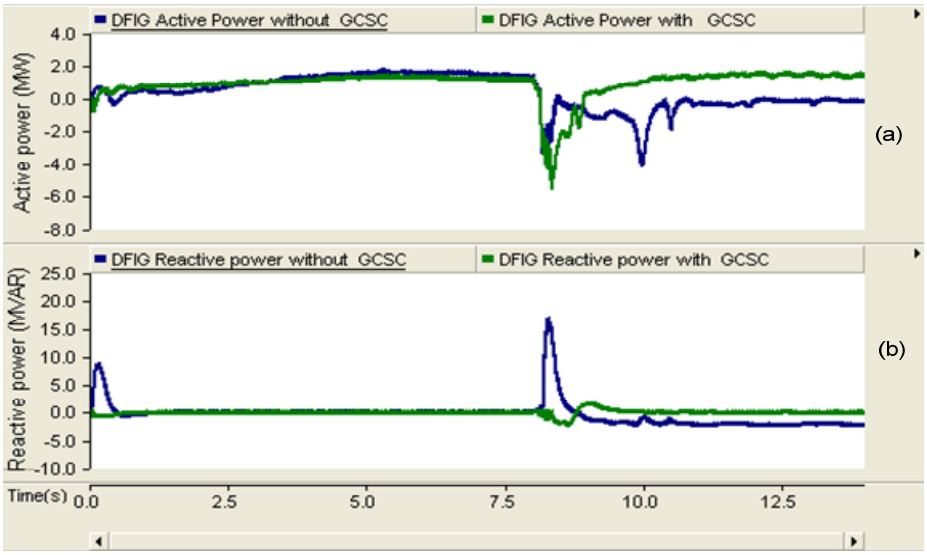

Figure 9. DFIG Power Response : (a) active power (b) reactive power

On the other hand, the DFIG electromagnetic torque and mechanical torque are presented in Figure 10(a) and (b). From Figure 10(a), the T_e without GCSC after fault clearing contains higher values because the rotor current is very high, which may be led to shaft fatigue whilst with GCSC is more stable and no dangerous to the shaft turbine system. The mechanical torque T_m follows the same behavior of T_e at a steady state, but after transient there is a big difference between them, which lead to abnormal system operation. In additional, the interesting result is to take the electromagnetic torque signal and analysis it by using on-line scanner frequency. This essentially used fast Fourier transform to get the harmonic frequency of the (T_e) as in Figure 11. From this figure, the maximum harmonic frequency of the T_e without GCSC is about 44.3974Hz which indicates that the SSR was happening in this system, but when the GCSC was added to the system, the frequency less than 1Hz. Regarding to these results, the SSR phenomenon was occurring in the system case study, and the GCSC mitigated the SSR effect.

The most important results are the shaft model system curves which are illustrated in Figure 12(a)-(c). Figure 12(a) shows the torque between mass2-1 T_{12}, Figure 12(b) the torque between mass3-2 T_{23}, and Figure 12(c) the torque between mass3-4 T_{34}. From these figures, the shaft torques with GCSC are stable and the oscillation produced from SSR has been damped.

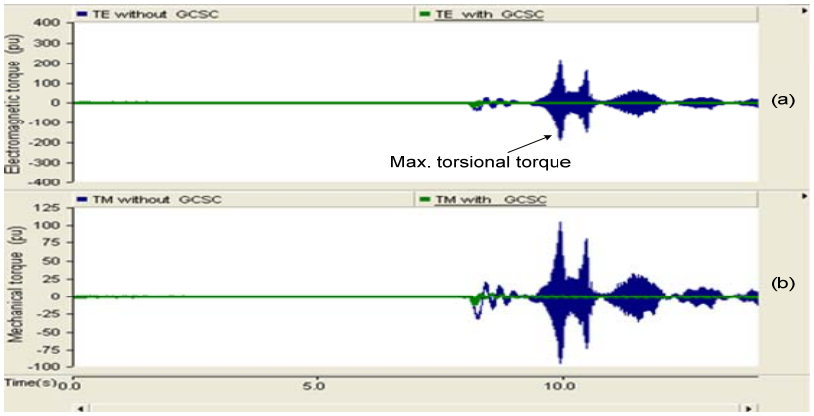

Figure 10. DFIG T_e and T_m Simulation Results: (a) electromagnetic torque T_e (b) mechanical torque T_m

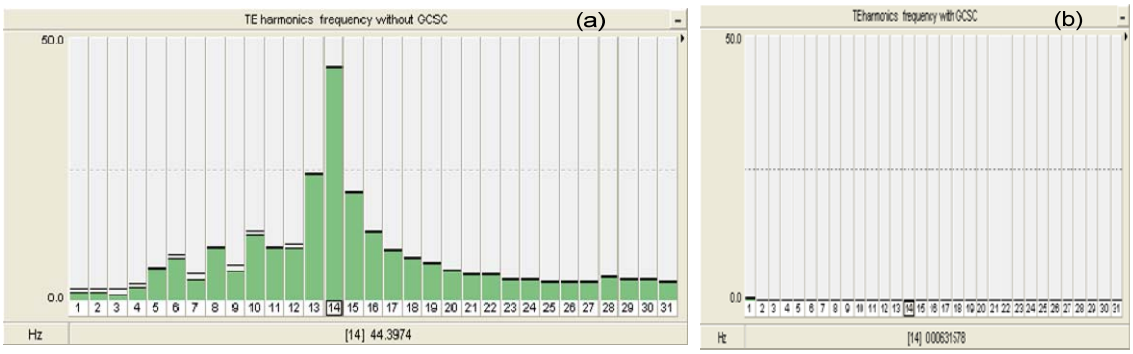

Figure 11. Electromagnetic Torque (T_e) Frequency Harmonics using On-line Scanner Frequency (fast Fourier transform FFT): (a) without GCSC; (b) with GCSC

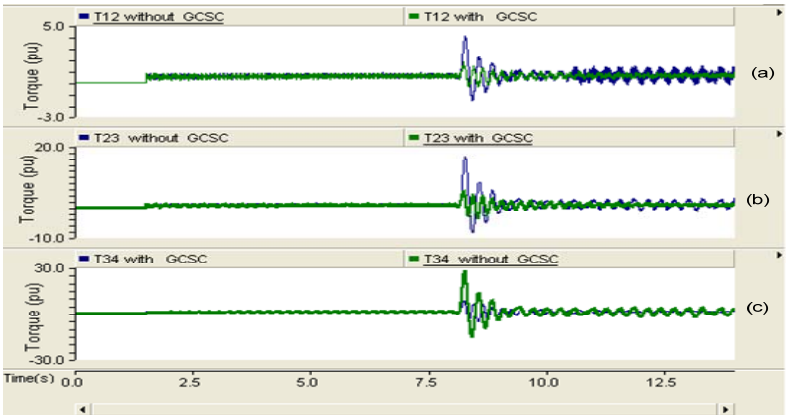

Figure 12. Shaft Model Results: (a) Torque between $mass_{1-2}$ T_{12} (b) Torque between $mass_{2-3}$ T_{23} (c) Torque between $mass_{3-4}$ T_{34}

The rotor speed without GCSC after fault clearing is going to zero, and the DFIG lost the synchronism which led to a different mode operation, but when we add the GCSC, the rotor speed transient response is improved. Figure 13(a) shows this behavior. Regarding to this result the rotor active power is varied according to the this speed, as in Figure 13(b).

Due to this operation, the DFIG voltage, PCC frequency and line phase current are directly affected. Their results are depicted in Figure 14(a)-(c) respectively. The DFIG recovery voltage (RV) without GCSC is very high (approximately is 9.0pu) because the potential energy in the inductance and capacitance are active, which lead to increase voltage and current dynamically in specific time. However, when the GCSC is operated all these parameters are under control.

The SSR problem is deeply affected to system elements such as DFIG converter parameters in both rotor and stator sides. For instant, rotor effective current, rotor q-axis reference current i_{rq_ref} , rotor d-axis reference current i_{rd_ref} and DC link voltage E_{cap} and they graphically illustrated in Figure 15(a)-(d) respectively.

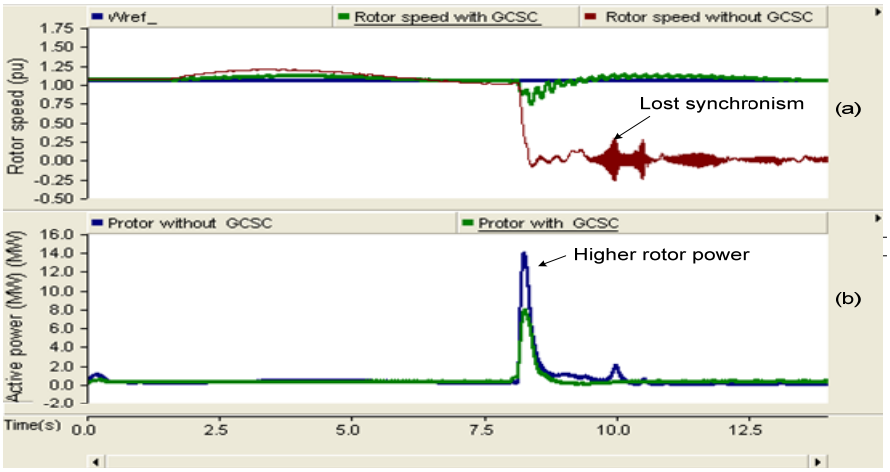

Figure 13. Rotor Side Results: (a) rotor speed ω_{pu} (b) rotor active power P_r

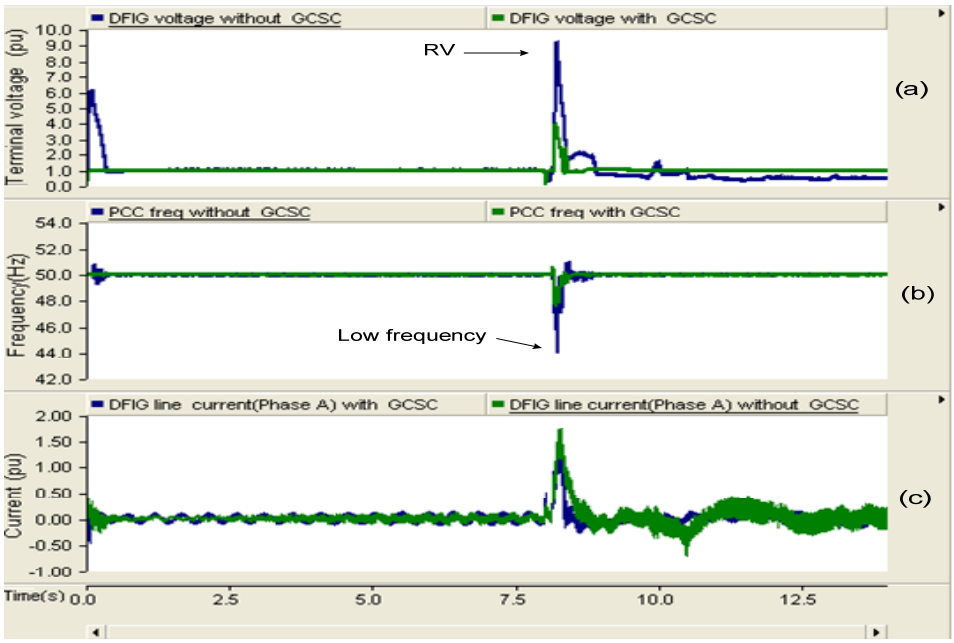

Figure 14. GS Results: (a) DFIG voltage (b) PCC frequency (c) DFIG phase current i_a

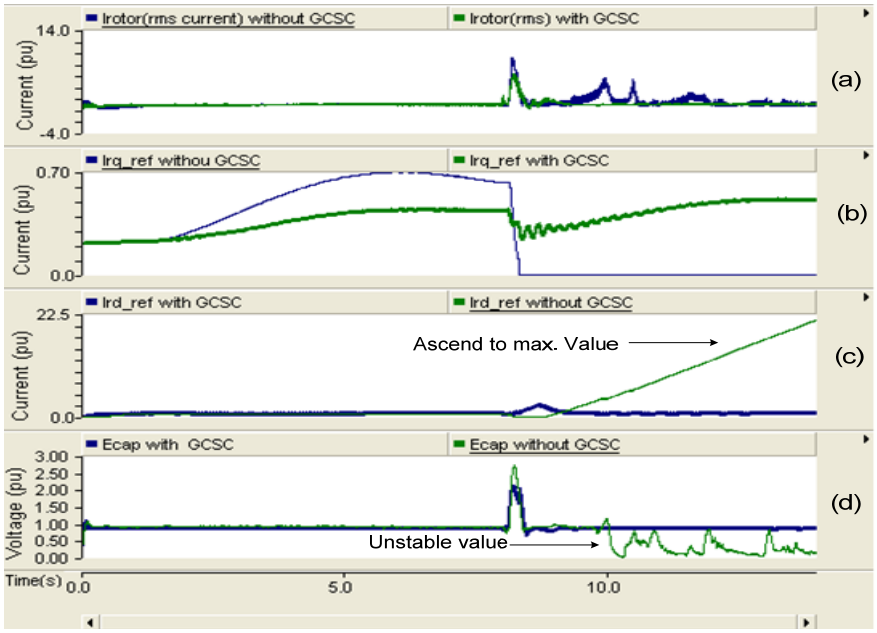

Figure 15. Converters Results: (a) rotor effective current (b) rotor q-axis reference current i_{rq_ref} (c) rotor d-axis reference current i_{rd_ref} (d) DC link voltage E_{cap}

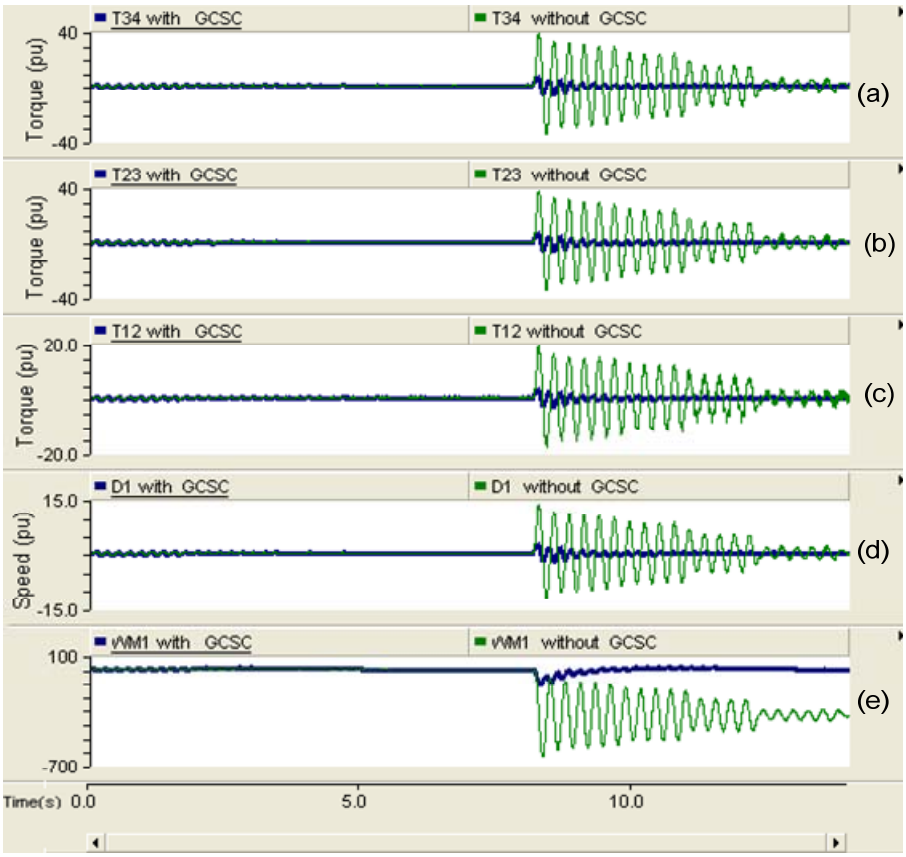

Figure 16. Shaft Model Results: (a) Torque between $mass_{3\text{-}4}$ T_{34} (b) Torque between $mass_{2\text{-}3}$ T_{23} (c) Torque between $mass_{1\text{-}2}$ T_{12} (d) mechanical position of $mass_1$ with respect to $mass_4$ (generator) D_1 (e) Delta mech. speed of $mass_1$ ω_{m1}.

From the above discussion, it is concluded that the DFIG in the system case study was lost the synchronism when it operates without GCSC in the dynamic model even there are some parameters did not lose the stability, but they operated in risk stability. The analysis indicates that system in the case study is faced the potential SSR problems type torsional interaction and its alleviated by a GCSC device .Therefore, GCSC device is very important to install in the system case study to mitigate the SSR problems during abnormal operation to improve the system stability as well. This model study can be extended to a large wind power system with a long transmission line to confirm the GCSC ability for mitigating SSR and the problems related to it. Moreover, the GCSC also has an ability to mitigate the subsynchronous oscillation (SSO) which happens during the SSR phenomenon when the transient mode occurred in the system. This issue can be explained graphically in Figure 16(a)-(e). This result is obtained from the shaft turbine model by increasing the fault duration time to let the system be more oscillating in order to check the GCSC ability for damping SSO, which associated with the SSR problems.

Generally, The mitigation of SSR by a GCSC is limited by changing the resonance frequency as compared to a fixed capacitor. This may not be adequate and Subsynchronous Damping controller (SSDC) may have to be used as a supplementary controller to damp subsynchronous oscillations.

10. Conclusion

In this paper, a novel SSR mitigation method based on GCSC in DFIG with series connected compensator is presented. This study explained that the GCSC could suppress SSR problems as well as improve system subsynchronous oscillation by using a approach control method. The comparison simulation results between a system study with and without GCSC show that the GCSC upgrade system stability even without specific control of the thyristor firing angles. Furthermore, the GCSC is very effective and reliable for operating as a compensated device in the power system with series compensator, which mainly used to improve the power capabilities of the transmission line. These results also show the ability of the GCSC to mitigate the SSO associated to the SSR problems. Without GCSC, the system completely lost synchronism after the fault clearing where the DFIG received active power from the general network, and all control parameters became instable. However, when the GCSC is added to the system, the DFIG return to stability as soon as and the system, dynamic performance is improved. The basic concept behind the GCSC operating is to change the system reactance during the fault according to the inrush current passes through the capacitor by applying a proper control for firing angle.

It notices here, the GCSC may be a more natural solution for the series compensation than the TCSC and SSSC which they have limited operations.

The author thinks that the main important factors of the SSR mitigation using GCSC could be written as:

a) The fault duration time must be out of the system time response range and less than the circuit breaker operation time, to allow the system returned to stability again. Otherwise, the system may be returned to stability but in risk operation.
b) The adjusted firing angle of GCSC value is more significant, and it plays a great role in the GCSC firing angle control (the suitable range less than 90°).
c) The GCSC capacitor value is directly associated to the series capacitor compensator, so it gives a percentage value according to the series capacitor value (in this study is about 80% of Xc).

The authors believe that, the GCSC may be competing in the SSR mitigation in the wind power system with series compensator when the large DFIG penetration into the system. But the GCSC needs more specific studies to confirm the approach control of the thyristor firing angles.

References

[1] Katz E, Chairman, Tang J. Comparison of SSR calculation and test results. *IEEE Transactions on Power Systems*. 1989; 4(1): 336-344.

[2] Zhu C, Fan L, Hu M. *Control and Analysis of DFIG-Based Wind Turbines in a Series compensated Network for SSR Damping.* Power and Energy Society General Meeting, IEEE. Minneapolis, MN: IEEE. 2010; 1 - 6.
[3] Fan L, Kavasseri R, Miao ZL, Zhu C. Modeling of DFIG-Based Wind Farms for SSR Analysis. IEEE Transaction on Power Systems. 2010; 25(4):2073-2082.
[4] Zhu C, Fan L, Hu M. Modeling and Simulation of a DFIG-Based Wind Turbine for SSR. North American Power Symposium (NAPS) Starkville, MS, USA: IEEE. 2009; 1 - 6.
[5] Atayde S, Chandra A. *Multiple machine representation of DFIG-based grid-connected wind farms for SSR studies.* IECON 2011 - 37th Annual Conference on IEEE Industrial Electronics Society; Melbourne, VIC: IEEE. 2011; 1468 - 1473.
[6] Zheng X, Zhang J, Wang C. Active Damping Controller Design for SSSC to Mitigate Subsynchronous Resonance. 2010.
[7] Thirumalaivasan R, Janaki M, Prabhu N.Damping of SSR Using Subsynchronous Current Suppressor With SSSC. *IEEE Transaction on Power Systems.* 2013; 28(1): 64 - 74.
[8] Vuorenpaa P, Rauhala T, Jarventausta P. *Applying TCSC Frequency Response Data Derived Using Electromagnetic Transient Analysis in SSR Frequency Scanning Studies*. PowerTech; Bucharest: IEEE Bucharest; 2009; 1-6.
[9] Hossein H, Behrooz T. Mitigating SSR in Hybrid System with Steam and Wind Turbine by TCSC. *Electrical Power Distribution Networks Tehran, IEEE.* Iran. 2012; 1-6.
[10] I Erlich, M Wilch, Feltes C. Reactive Power Generation by DFIG Based Wind Farms with AC Grid Connection. *Power Electronics and Applications Conference European- Aalborg: IEEE.* 2007; 1-10.
[11] Johansson N, Ängquist L, Nee H-P. A Comparison of Different Frequency Scanning Methods for Study of Subsynchronous Resonance. *IEEE Transaction on Power Systems*. 2011; 26(1): 356-363.
[12] Zhi-qiang Z, M XX-n. Analysis and Mitigation of SSR Based on SVC in Series Compensated System. *Energy and Environment Technology,* ICEET Guilin, Guangxi, China: IEEE. 2009; 65-68.
[13] El-Moursi MS, Bak-Jensen B, Abdel-Rahman MH. Novel STATCOM Controller for Mitigating SSR and Damping Power System Oscillations in a Series CompensatedWind Park. *IEEE Transaction on Power Electronics*. 2010; 25 (2): 429- 441.
[14] Golshannavaz S, Mokhtari M, Nazarpour D. *SSR suppression via STATCOM in series compensated wind farm integrations*. International Conference of Electrical Engineering (ICEE); Tehran, Iran: IEEE. 2011; 1-6.
[15] Watanabe EH, Souza LFWd, Jesus FDd, Alves JER, Bianco A. *GCSC - Gate Controlled Series Capacitor: a New Facts Device for Series Compensation of Transmission Lines*. IEEE/PES Transmission & Distribution Conference & Exposition; Latin America: IEEE. 2004; 1-6.
[16] Jesus FDd, Hirokazu Watanabe E, Souza LFd, José Eduardo R. Alves J. SSR and Power Oscillation Damping Using Gate-Controlled Series Capacitors (GCSC). *IEEE Transaction on Power Delivery*. 2007; 22(3): 1806-1812.
[17] I Group ISW. *Proposed Terms and Definitions for Subsynchronous Resonance IEEE Symposium on Countermeasures for Subsynchronous Resonance*. IEEE Symposium on Countermeasures for Subsynchronous resonance. 1981; IEEE Pub. 81TH0086-9-PWR:92-97.
[18] Bongiorno M, Ängquist L, Svensson J. A Novel Control Strategy for Subsynchronous Resonance Mitigation Using SSSC. *IEEE Transaction on Power Delivery*. 2008; 23(2): 1033-1041.
[19] Fan L, Miao Z. Mitigating SSR Using DFIG-Based Wind Generation. *IEEE Transaction on Sustainable Energy*. 2012; 3(3): 349-358.
[20] BinWu, Yongqiang Lang, Navid Zargari, S Kouro. *Power conversion and control of wind energy systems*. Hoboken, New Jersey: John Wiley & Sons, Inc. 2011.
[21] Eftichios Koutroulis, Kalaitzakis K. Design of a Maximum Power Tracking System for Wind-Energy-Conversion Applications. *IEEE Transaction on Industrial Electronics*. 2006; 53(2): 486-494.
[22] Orlando S, Henrique G, António M, Adriano C. Nonlinear control of the doubly-fed induction generator in wind power systems. *Renewable Energy*. 2010; 35(8): 1662-1670.
[23] Okedu KE. A Study of Wind Farm Stabilization Using DFIG or STATCOM Considering Grid Requirements. *Engineering Science and Technology Review*. 2010; 3(1): 200-209.
[24] Slootweg JG, Haan SWHd, Polinder H, Kling WL. General Model for Representing Variable Speed Wind Turbines in Power System Dynamics Simulations. *IEEE Transaction on power systems*. 2003; 18(1): 144-151.
[25] Gonzalo Abad, Jesús López, Miguel A Rodríguez, Luis Marroyo, Iwanski G. *Doubly Fed Induction Machine Modeling and Control for Wind Energy Generation Applications.* Hoboken, New Jersey: John Wiley & Sons, Inc; 2011.
[26] Alvaro Luna, Francisco Kleber de Araujo Lima, David Santos PR, Edson H. Watanabe, Arnaltes S. Simplified Modeling of a DFIG for Transient Studies in Wind Power Applications. *IEEE Transaction on Industrial Electronics*. 2011; 58(1): 9-20.
[27] B Rabelo, W Hofmann JL Silva, RG Oliveira, Silva SR. Reactive Power Control in Doubly-Fed Induction Generators for Wind Turbines. *Power Electronics Specialists Conference(PESC) Rhodes: IEEE*. 2008; 106-112.

[28] Jiyong Zhang, Liu G. Control for Wind Power Generation based on Inverse System Theory. *TELKOMNIKA Indonesian Journal of Electrical Engineering.* 2013; 11(11): 6815-6824.
[29] Li S, Haskew TA. Analysis of Decoupled d-q Vector Control in DFIG Back-to-Back PWM Converter. In: IEEE, editor. *Power Engineering Society General Meeting*; Tampa, FL: IEEE. 2007; 1 - 7
[30] Li S, Haskew TA, Hong Y-K, Xu L. Direct-current vector control of three-phase grid-connected rectifier–inverter. *Electric Power Systems Research.* 2011; 81(2): 357-66.
[31] Huang Wang-jun, Zeng Zhi-gang, Zhou Hui-fang, Ten Yuan-jiang, Li L. Modeling and Experimental Study on Grid- Connected Inverter for Direct Drive Wind Turbine. *TELKOMNIKA Indonesian Journal of Electrical Engineering.* 2013;11(4): 2064-2072.
[32] M Mohseni, S Islam, Masoum MAS. Fault ride-through capability enhancement of doubly-fed induction wind generators. *IET Renewable Power Genereration.* 2011; 5(5): 368–376.
[33] SM Muyeen, Junji Tamura, Murata T. *Stability Augmentation of a Grid-connected Wind Farm*. Springer-Verlag London Limited; 2009.
[34] Xiaojin Z, Xiaorong X. A Multimass Model With Non-Linear Modal Damping For SSR Analysis Of Turbine-Generators. Sustainable Power Generation and Supply, Nanjing- China: IEEE. 2009; 1 - 5.
[35] PM Anderson, BL Agrawal, Ness JEV. Subsynchronous Resonance in power systems. New York: Wiley-IEEE press; 1990.
[36] Narain G Hingoranl, Gyugyi L. Understanding Facts Concepts and Technology of Flexible AC Transmission Systems. New York: A John Wiley & Sons, INC.; 2000.
[37] Souza LFWd, HirokazuWatanabe E, José Eduardo da Rocha Alves J. Thyristor and Gate-Controlled Series Capacitors: A Comparison of Components Rating. *IEEE Transaction on Power Delivery*. 2008; 23(2): 899-906.
[38] Luiz FelipeWillcox de Souza, Edson Hirokazu Watanabe, Aredes M. GTO Controlled Series Capacitors: Multi-Module and Multi-Pulse Arrangements. *IEEE Transactions on Power Delivery*. 2000; 15(2): 725 -731.

Appendix

Table 1. DFIG Parameters and System Data

1.5 MW DFIG		**Network system**	
Rated power	1.5 MW	Transformer ratio	0.69/20 kV
Rated voltage	690 V	Rated power	1.5 MVA
Rated frequency	50 Hz	Line voltage	20 kV
Number of pole pairs, p	2.0	Line length	80 km
Stator winding resistance, R_s	0.0084 pu	Transmission line parameters were adopted	
Rotor winding resistance, R_r	0.0083 pu	from PSCAD library as	
Stator leakage inductance, L_{Ls}	0.167 pu	total X=27.98Ω, K=0.5,	
Rotor leakage inductance, L_{Lr}	0.1323 pu	Capacitance, X_C	13.99Ω (227.5μF)
Magnetizing inductance, L_m	5.419 pu	nductance ,X_L	19.98Ω (0.0636H)
Inertia constant, H	1.1 s	Resistance, R_L	1.015Ω
DC link capacitance	9800 μF	DC link base voltage	1200 V

Table 2. Pitch Angle Controller Data

Wind turbine		**Pitch controller parameters**	
Rated power, P_m	1.5 MW	Proportional gain, K_p	3.2°/ pu
Rotor radius, R	40 m	Integral gain, K_i	6.2 °/ pu
Air density, ρ	1.229 kg/m^3	Initial pitch angle, β_0	7.5°
Gearbox ratio	60	Blade actuator integral gain, K4	0.9 s
Gearbox efficiency	0.97 pu	Blade actuator rate	10°/s
Average wind speed, V_w	11.42 m/s		

Table 3. Shaft System Parameters

H_1	0.122sec	H_2	0.4674sec
H_3	0.5184sec	K_{12}	19.7pu
K_{23}	20.8pu	K_{34}	25.2pu
D_{12}	0.006pu	D_{23}	0.006pu
D_{34}	0.006pu		